● *Original Contribution*

HIGH-FRAME-RATE POWER DOPPLER ULTRASOUND IS MORE SENSITIVE THAN CONVENTIONAL POWER DOPPLER IN DETECTING RHEUMATIC VASCULARISATION

MYRTHE VAN DER VEN,* JOLANDA J. LUIME,* LEVINIA L. VAN DER VELDEN,* JOHAN G. BOSCH,[†] JOHANNA M. W. HAZES,* and HENDRIK J. VOS[†]

*Department of Rheumatology, Erasmus MC, Rotterdam, The Netherlands; and [†]Department of Biomedical Engineering, Thoraxcenter, Erasmus MC, Rotterdam, The Netherlands

Abstract—Early recognition of joint inflammation will increase treatment efficacy in rheumatoid arthritis (RA). Yet, conventional power Doppler (PD) ultrasound might not be sufficiently sensitive to detect minor inflammation. We investigated the sensitivity of high-frame rate Doppler, combined with singular value decomposition technique, to suppress tissue signals, for microvascular flow in a flow phantom setup and in a proof-of-principle study in healthy controls and in RA patients with different disease activities. In the flow phantom, minimal detectable flow velocity was a factor 3 lower with high-frame-rate PD than with conventional PD ultrasound. In the proof-of-principle study we detected a positive PD signal in all volunteers, diseased or healthy, with high-frame-rate PD ultrasound. We saw a gradual increase in PD signal in RA patients depending on disease activity. In conclusion, high-frame rate Doppler is more sensitive in detecting vascularisation than conventional PD ultrasound. (E-mail: h.vos@erasmusmc.nl)   © 2017 The Authors. Published by Elsevier Inc. on behalf of World Federation for Ultrasound in Medicine & Biology. This is an open access article under the CC BY-NC-ND license (http://creativecommons.org/licenses/by-nc-nd/4.0/).

Key Words: Subclinical rheumatoid arthritis, Echography, Plane wave imaging, Power Doppler, Singular value decomposition.

INTRODUCTION

Rheumatoid arthritis (RA) is an inflammatory joint disease with a prevalence of 1% worldwide (Silman and Pearson 2002). RA leads to destruction of joints, severe disability and increased cardiovascular mortality (McInnes and Schett 2011). Obligatory for the current diagnosis of RA is inflammatory arthritis of at least one joint (Aletaha et al. 2010). Arthritis is assessed by manual palpation of swelling in joints. Treatment of RA is directed at suppressing inflammation and establishing a state of remission according to a treat-to-target protocol (Stoffer et al. 2015; van Nies et al. 2014). Remission is regarded as the ultimate therapeutic goal for RA patients to prevent further joint damage and disability and to maintain function and quality of life. Therefore, it is important to ensure that the methods of assessing disease activity are accurate to diagnose and monitor

RA. Current clinical measures rely on composite scores based on physical examination (swollen and tender joints) and laboratory assessments (Prevoo et al. 1995; Smolen et al. 1995). These measures have the disadvantage of not directly measuring inflammation and may be subject to confounding influences and subjectivity. In addition, reports suggest a disparity between clinical status and outcome, with evidence of radiographic or cytoscopic progression despite apparent clinical remission (Andersen et al. 2014; Brown et al. 2006; Kitchen and Kane 2015). This indicates ongoing subclinical inflammation. Data from several ultrasound studies indicate that subclinical disease lingers in joints that lack clinical signs of arthritis (Brown et al. 2008; Filer et al. 2011; Yoshimi et al. 2013). Presence of subclinical disease may explain why some patients still develop bone erosions or have a relapse of their disease, while clinically the disease is in remission (Brown et al. 2008; Peluso et al. 2011; Saleem et al. 2012; Scire et al. 2009; Yoshimi et al. 2013).

A review from Ten Cate et al. (2013a) revealed that ultrasound imaging, especially use of the power

---

Address correspondence to: Hendrik J. Vos, Department of Biomedical Engineering, Thoraxcenter, Erasmus MC, Ee2318, PO Box 2040, 3000 CA Rotterdam, The Netherlands. E-mail: h.vos@erasmusmc.nl

Doppler (PD) mode, has added value in the diagnosis of RA and the monitoring of RA patients who are in remission. In conventional ultrasound, any PD signal in the joint indicates elevated vascularisation, which is an important sign of active inflammation. Conventional PD modes can detect flow velocities down to 0.05 mm/s in a flow phantom experiment in which the background tissue is motionless, although there is a large variability between ultrasound machines in the sensitivity to detect low flows (Ten Cate et al. 2013b). In actual clinical application, the settings used in these phantom experiments produce flash artefacts—caused by unavoidable minor motion—which fully cover the blood signal. To be able to detect low flow velocities in actual clinical application there is a need for a sensitive PD ultrasound modality that reduces such flash artefacts.

In the past decade, high-frame-rate ultrasound has improved sensitivity to blood flow (Tanter and Fink 2014; Bercoff et al. 2011). With high-frame-rate ultrasound, the entire field of view is imaged with a single transmission, enabled by advances in the electronic hardware of the ultrasound machines. The high frame rate ensures high temporal correlation between frames, which facilitates a good separation between relatively slow tissue motion and blood flow (Maresca et al. 2014; Tanter and Fink 2014). This has led to the improved sensitivity of blood flow imaging in, for example, rheumatology (Maresca et al. 2014; Tanter and Fink 2014), brain vascular imaging (Demené et al. 2014, 2016) and carotid flow velocity estimation (Ekroll et al. 2015; Hasegawa and Kanai 2008; Lenge et al. 2014). The high temporal correlation between frames also allows for use of spatial correlation to further discriminate blood flow in small localised vessels from global motion of soft tissue and bone, generally enabled with singular value decomposition (SVD) (Demené et al. 2015; Song et al. 2017).

We applied the combination of high-frame-rate Doppler ultrasound imaging and SVD filtering, which is expected to be more sensitive to low flow velocities than the conventional method (Demené et al. 2015), for perfusion imaging of finger joints. It is our premise that such a more sensitive technique can provide accurate detection of active inflammatory joint tissue in RA, enabling earlier diagnosis of RA and better treatment monitoring. Of note, an early diagnosis of RA assumes that the patient is frequently seen by a rheumatologist. This is the case because the persons have inflammatory joint complaints, albeit without clinically apparent swollen joints and, so, according to clinical decision diagrams, do not get the diagnosis of RA at that point. In such cases, sensitive PD ultrasound would be able to improve diagnostic accuracy.

In this study, our first aim was to determine, in a flow phantom, if the high-frame-rate Doppler ultrasound technique is more sensitive in detecting low flows than a conventional clinical ultrasound machine. Our second aim was to perform a proof-of-principle study in RA patients with varying disease activity to evaluate whether we are able to detect higher levels of vascularisation in affected joints with the new technique than with the conventional method. The proof-of-principle study was complemented with healthy volunteers to evaluate to what level healthy joints show vascularisation.

METHODS

Flow phantom

The flow phantom (Fig. 1) consisted of an acrylic (polymethyl methacrylate) container filled with tissue-mimicking material, according to a previously published recipe (Teirlinck et al. 1998). In this tissue-mimicking material we placed a 0.7-mm (inner diameter) microvessel made of silicone (Eriks, Alkmaar, Netherlands). Evaluation of the vessels was at a depth of 8–10 mm, which would be the largest depth of possible vessels in the metacarpophalangeal (MCP) joint under study. A blood-mimicking fluid (BMF) was prepared based on the recipe of Ramnarine et al. (1998). The BMF contained 91% (w/w) demineralised water, 1% (w/w) dextran (average 150 kDa, D4876, Sigma-Aldrich, Zwijndrecht, Netherlands), 1% (w/w) ICI supersonic N surfactant, 5% (w/w) glycerol and 2% w/w Orgasol particles (5 μm in diameter, Arkema, Rotterdam, Netherlands). The BMF was mixed using a magnetic stirrer, filtered using a 40-μm sieve (352340, BD, Breda, Netherlands) and degassed using a vacuum pump. Compared with the original recipe of Ramnarine et al., our BMF contained half the amount of dextran and glycerol; this made our BMF less viscous, which was necessary to prevent blockage of the vessels. A syringe pump (Hugo Sachs Elektronik, March-Hugstetten, Germany) was used to generate flows. We calculated flow settings that corresponded to average flow velocities ranging from 26 to 0.13 mm/s, using the equation

$$Q = V_{avg} \times \pi R^2 \qquad (1)$$

where Q is flow (m^3/s), V_{avg} is average flow velocity (m/s) and R is the inner radius (m). On assumption of a parabolic flow profile, the peak velocity is twice the average velocity in a circular tube (Evans and McDicken 1999). Reported velocities are peak velocities.

Study population

Ten healthy controls and 14 RA patients were included in this proof-of-principle study. To be able to interpret ultrasound results, we included RA patients
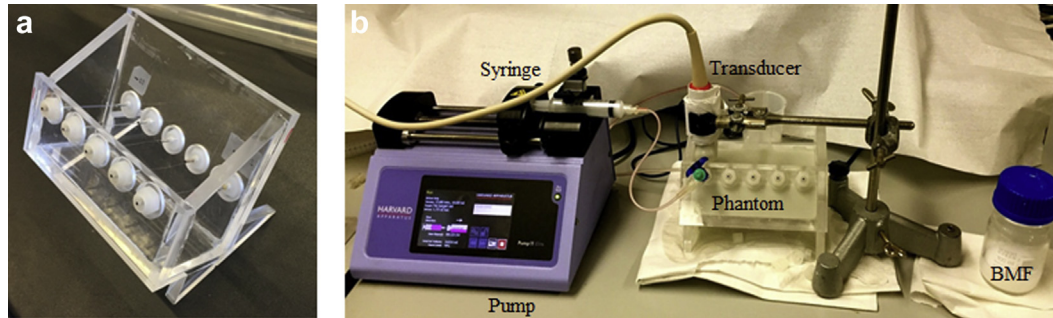
Fig. 1. (a) Flow phantom before actual filling the cavity with tissue-mimicking material. (b) Experimental phantom setup; BMF= blood-mimicking fluid.

with a broad spectrum of disease activity: (i) RA patients in clinical remission (no clinically swollen or tender joints); (ii) RA patients who were well controlled (low to medium disease activity, but with clinically swollen and/or tender joints); and (iii) RA patients with a clinical flare (high disease activity with clinically swollen and/or tender joints). Disease activity was measured by physical examination of swollen and tender joints, and the disease activity score in 28 joints (DAS28) was calculated (Prevoo et al. 1995). A clinically swollen joint needed to be confirmed by the patient's treating rheumatologist. Written informed consent was obtained from the participants according to the Declaration of Helsinki. The study was approved by the local medical ethics committee of Erasmus MC, University Medical Centre Rotterdam, The Netherlands (MEC-2015-179).

Ultrasound equipment and machine settings

Conventional ultrasound machine. The conventional ultrasound machine was an Esaote MyLab60, which is used in daily clinical practice, and was equipped with a high-frequency linear array probe (LA435, 10-18 MHz). In both the phantom and clinical studies, the probe was mounted on a 4-degree-of-freedom mounting arm with a hydrostatic brake (442110/290 mm, Noga Engineering, Noga, Israel) to reduce probe motion caused by the sonographer. To reduce the motion of the hand of the participant, the hand was positioned in a custom plate with pins to spread the fingers (Fig. 2). Participants were sitting on a chair and were asked to hold their breath (after breathing out) during the measurement to reduce residual motion as much as possible. The PD gain was set at the disappearance level of colour noise in the PD images. The pulse repetition frequency (PRF) was set as low as possible to have maximum sensitivity for low flow, which was 125 Hz in the phantom study and 750 Hz in the clinical pilot study. Further settings are listed in Table 1.

We adjusted the size and position of the colour box to include the subcutaneous tissue to recognise artefacts caused by vessels above the joint (Torp-Pedersen and Terslev 2008).

Research ultrasound machine. The research system was a Vantage-256 (Verasonics, Kirkland, WA, USA) with a high-frequency probe (L40-8/12, Ultrasonix, Richmond, BC, Canada) with a customised adapter to the Verasonics system. The specifications of this probe are equal to those of the Verasonics L22-14v probe. The system was programmed in high-frame-rate mode, that is, plane wave transmissions, and capturing and saving the full channel data (Maresca et al. 2014). One B-mode image and one Doppler ensemble were recorded per data set. The Doppler ensemble consisted of 122 frames in in-phase quadrature (IQ) format. Each Doppler frame was composed of coherent summation of the images reconstructed from 11 angled plane wave transmit/receive events, transmitting over an angular range of $-10°$ to $+10°$. The image reconstruction was performed by
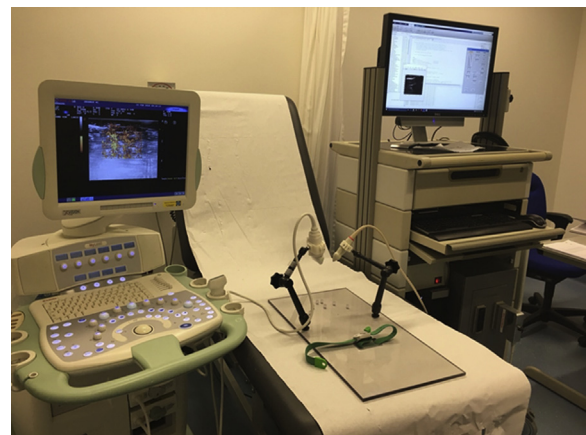

Fig. 2. Experimental setup for the proof-of-principle study with the probe-mounting arms and the custom plate with pins to spread and fixate the fingers. Left machine: Esaote MyLab 60, right machine: Verasonics Vantage-256 on a custom trolley.

Table 1. Conventional ultrasound (Esaote MyLab60) settings for the phantom study and the proof-of-principle study

	Phantom study	Proof-of-principle study
Doppler frequency (MHz)	10	10
Pulse repetition frequency (Hz)	125	750
Wall filter	Level 1	Level 3
Power Doppler persistence	Level 4	Level 4
Image depth (cm)	3.0	2.5

the internal Verasonics reconstruction algorithm. The ultrasound pulse was a 1-cycle tone burst at 12.5 MHz for the B-mode and a 4-cycle tone burst at 12.5 MHz for the Doppler data. The PRF was set to 1375 pulses/s, resulting in a rate of 125 frames/s in the Doppler ensemble. This led to the recording time of approximately 1 s, that is, one Doppler image per second. Given a general heart rate of one beat per second, this recording time implies that the PD signal is obtained over one complete heart cycle, and no diastolic or systolic difference is observed, unlike regular PD which has image rates of a few per second.

The performance of the high-frame-rate imaging was tested in a flow phantom. In this experiment, we used a Doppler frame rate of 500 Hz and 62 frames, resulting in a recording time of 124 ms. Such a Doppler ensemble recording time is closer to that of the image rate in the clinical scanner. This measurement served as an initial test to illustrate the higher sensitivity to low flow velocities of the high-frame-rate imaging in a controlled environment.

To investigate the influence of wall filters, we tested both a conventional wall filter with static high-pass filtering characteristics and the recent approach of SVD according to the procedure of Demené et al. (2015). In the phantom study, the conventional wall filter (Verasonics built-in filter WeakFlowVLow) had −6- and −20-dB cutoff frequencies of 12 and 6 Hz, respectively, which results in a cutoff velocity of 0.4–0.8 mm/s. In the study with volunteers, we used a sixth-order zero-phase Butterworth filter with a –6-dB cutoff frequency of 37.5 Hz, which results in a cutoff velocity of 2.4 mm/s. Lower cutoff frequencies led to severe flash artefacts. The SVD filtering is a statistical approach in which high-amplitude tissue signals with large spatial coherency are separated from the low-amplitude local blood signals, and then removed. Moreover, electronic noise is separated and subsequently removed by the filter, because noise has low amplitude and very low spatial coherency. The lower separation threshold (for tissue suppression) was manually set to visually suppress tissue signals and quasi-static signals

from the bone structure, while maintaining the blood signal in the PD image (Demené et al. 2015). The higher separation threshold (for noise suppression) was manually set to suppress the noise signal in the deeper regions of the image, where no ultrasound echo would be expected because that region is located inside bone. This led to SVD cutoff values of 18 and 32, respectively (of a set of 122 frames). The power Doppler signal is then normalized to the maximum Doppler power value in the image. In the images, we overlay the Doppler power to the B-mode images. If the Doppler power in any pixel is larger than 12% of the maximum Doppler power in the image, then the pixel gets its Doppler power value; otherwise, the pixel gets the B-mode grey-scale value. Note that this procedure may be different from that for conventional power Doppler, in which the grey-scale value determines the local power Doppler sensitivity in the image (so-called colour priority), which enhances larger vessels in the power Doppler images that appear black on the grey-scale images. Such power Doppler enhancement by colour priority is not meaningful when the vessel diameters are smaller than the image resolution, which is generally the case in scanning the fine vasculature in the hand.

Imaging protocols

Phantom study. In the flow phantom, the lowest detectable flow for each machine and vessel was defined as the flow that still resulted in a continuous PD signal. The pump was set to a high flow and then decreased gradually until the PD signal disappeared. The value of the lowest flow was recorded, an image for each lowest detectable flow was stored and we recorded the machine settings used to acquire this image. Between changes in pump flow, we waited 5 min to reach stable flow velocities.

Proof-of-principle study. In the proof-of-principle study, we used the experimental setup in Figure 2 to position the probe and the hand according to EULAR guidelines (Backhaus et al. 2001). In healthy controls, MCP2 (second metacarpophalangeal joint, dorsal aspect) was ultrasonographically evaluated in extended position. In RA patients, two MCP joints were examined. In RA patients in clinical remission, bilateral MCP2 joints were examined. In RA patients who had controlled disease, a clinically swollen joint (MCP2 or MCP3) was examined. In this group, a clinically non-swollen joint (MCP2 or MCP3) was also examined and used as an in-patient reference joint. In RA patients with a clinical flare, two clinically swollen joints (MCP2 or MCP3) were examined. In all cases, each joint was evaluated three times by PD; the maximum score of three was the final score.

Ultrasound evaluation

The comparison of images by different modalities (conventional and high-frame rate) was evaluated semi-quantitatively, and the presence or absence of PD signal on each imaging modality was recorded. Synovial vascularisation was measured using PD. PD was graded as 0 = absent; 1 = mild single-vessel signal or isolated signal; 2 = moderate confluent vessels; and 3 = marked vessel signals in more than half of the intra-articular area (Szkudlarek et al. 2003).

The PD images acquired with high-frame-rate ultrasound were scored by four raters independently. Raters were blinded to all clinical information. For each image, the median of the PD scores was taken. To optimise inter-rater reliability, the raters followed a standardised protocol that instructed them to ignore any residual signal elicited at the bone surface and to ignore flash artefacts.

Statistical analysis

Simple descriptives were used to describe baseline characteristics and ultrasound findings. According to

general convention of median values, if there is an even number of items in the data set, then the median is taken as the average of the two middle numbers after sorting. We calculated the κ statistic (Viera and Garrett 2005) to determine the inter-rater reliability for scoring PD images acquired with high-frame-rate imaging.

We analysed differences in PD scores between the conventional ultrasound method and high-frame-rate imaging. Because the data were not normally distributed, we used the Wilcoxon–Mann–Whitney test. Analyses were done using STATA 14.0, with a p value ≤ 0.05 as the level of statistical significance.

RESULTS

Phantom study

In Figure 3 are the PD images obtained at the lowest detected velocities in the flow phantom. The high-frame-rate ultrasound machine detected minimal flow velocities of 0.5 mm/s with the conventional wall filter and 0.26 mm/s with the SVD-based wall filter. The conventional ultrasound machine detected a minimal flow
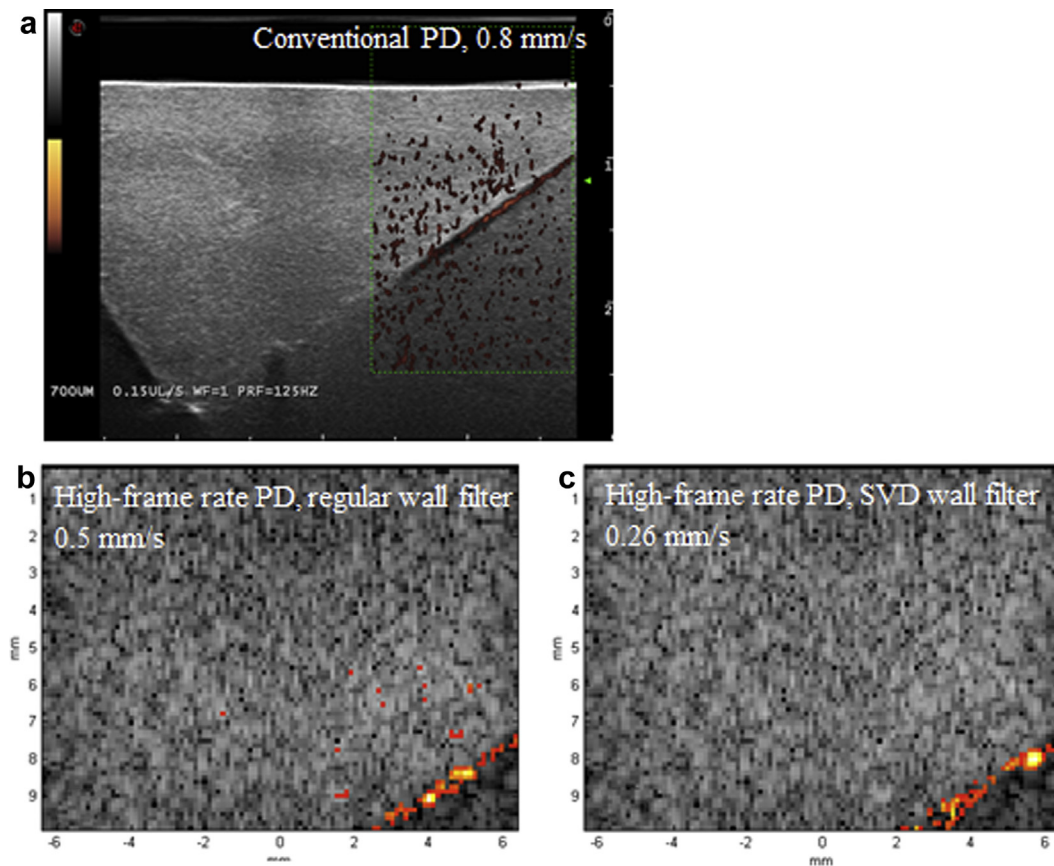

Fig. 3. Power Doppler images obtained in the 700-μm vessel at the lowest detected velocity with the respective machines and wall filtering. (a) Conventional PD ultrasound, lowest wall filter, and V_{peak} = 0.8 mm/s. (b) High-frame-rate Doppler, conventional wall filter and V_{peak} = 0.5 mm/s. (c) High-frame-rate Doppler, tissue filter based on singular value decomposition (SVD) and V_{peak} = 0.26 mm/s. PD = power Doppler.

velocity of 0.8 mm/s. Because the phantom and probe both had very low residual motion, the PRF and wall filter in the conventional ultrasound machine could be set extremely low, compared with regular clinical settings. In the current examination, the PRF was 125 Hz and the wall filter was set to level 1, which is the lowest setting. In regular clinical ultrasound, the minimal PRF to avoid flash artefacts is 750 Hz, and the wall filter, level 3. This implies that the lowest detectable flow velocity with the conventional ultrasound machine under clinical conditions is at least a factor of 6 higher (because of the factor of 6 increase in the PRF), which is 4.8 mm/s.

Proof-of-principle study

We included 10 healthy controls (mean age [range]: 32 [22–59] y) and 14 RA patients (58 [31–70] y), of whom 3 were in clinical remission, 9 were well controlled and 2 had a clinical flare. Baseline characteristics are summarised in Table 2.

Example images are provided in Figure 4. The left images are the screen shots of the conventional PD ultrasound, whereas the right images are the high-frame-rate Doppler ultrasound images. Images were taken of a healthy control (Fig. 4a,f) and RA patients in different disease states (Fig. 4b–e,g–j). The bone edges are identified by the bright inclined structures in the images at depths between 2 and 5 mm. The joint is presented by the V-shape of the bone, and the synovium of healthy joints is located at the top of the area bounded by the V-shape. In healthy joints, the synovium is very thin and thus not visible in ultrasound images; however, it may contain a small number of blood vessels because the synovial fluid (inside the synovium) is fed from the synovium. In rheumatoid arthritis, the synovium is thick and highly perfused because of inflammation of the surrounding area. In such cases, PD ultrasound should be able to measure significant blood signal.

Figure 4 illustrates these effects. The high-frame-rate Doppler images indicate more PD signal with increasing disease severity, whereas the conventional Doppler indicates a PD signal for the swollen joint and with clinical flare. Moreover, the high-frame-rate Doppler images also reveal a significant signal at the bone surfaces, where the cartilage is located. We presume that this is a PD artefact, caused by minor motion of the bone in combination with very large amplitude of the reflection signal. When scoring the PD signal, we neglected this signal at the location of the cartilage/bone surface.

Figure 4 also illustrates that the conventional imaging system has a high-quality grey-scale image, presumably caused by an interleaved ultrasound sequence to generate a grey-scale image and the Doppler image quasi-simultaneously. In our current implementation of the high-frame-rate sequence, we did not optimise for the grey-scale image quality; we used a quick angular plane wave compounding technique to produce the grey-scale image, at a quality that is sufficient to align the transducer in real time and sufficient to interpret the anatomic landmarks. In further clinical studies, this grey-scale acquisition sequence can be further optimized to reach regular clinical quality, to also score the disease state based on the grey-scale images.

With reference to Table 2, conventional PD ultrasound in healthy controls and in RA patients in clinical remission revealed no PD signal in MCP2 joints and either no or minimum signal in the non-swollen joints of RA patients. In the swollen joints of controlled RA patients and RA patients with a clinical flare, the median PD score was 1 (interquartile range [IQR]: 0–2).

With high-frame-rate PD ultrasound, the median PD score was 2 (IQR: 2–2) in healthy controls, 1.5 (IQR: 1–2) in RA patients in remission, 2 in controlled RA patients in both non-swollen (IQR: 2–2) and swollen (IQR: 1.5–2) MCP joints and 2 (IQR: 2–3) in RA patients with a flare

Table 2. Baseline characteristics and ultrasonographic findings

	Controls (n = 10)	RA remission (n = 3)	RA controlled (n = 9)		RA flare (n = 2)
Age, mean (range)	32 (22–59)	53 (48–59)	59 (31–70)		56–67
Female, %	60	100	78		100
DAS28, mean (range)		2.8 (2.7–3.0)	3.1 (1.3–4.2)		4.3–5.7
SJC, median (range)		0 (0–0)	5 (3–6)		1–11
TJC, median (range)		0 (0–0)	2 (0–3)		7–16
			Non-swollen MCP	Swollen MCP	
Conventional US					
PD score, median (IQR)	0 (0–0)	0 (0–0)	0 (0–1)	1 (0–2)	1 (0–2)
High-frame-rate US					
PD score, median (IQR)	2 (2–2)	1.5 (1–2)	2 (2–2)	2 (1.5–2)	2 (2–3)

DAS28 = disease activity score in 28 joints; SJC = swollen joint count; TJC = tender joint count; MCP = metacarpophalangeal joint; US = ultrasound; PD = power Doppler; IQR = interquartile range.
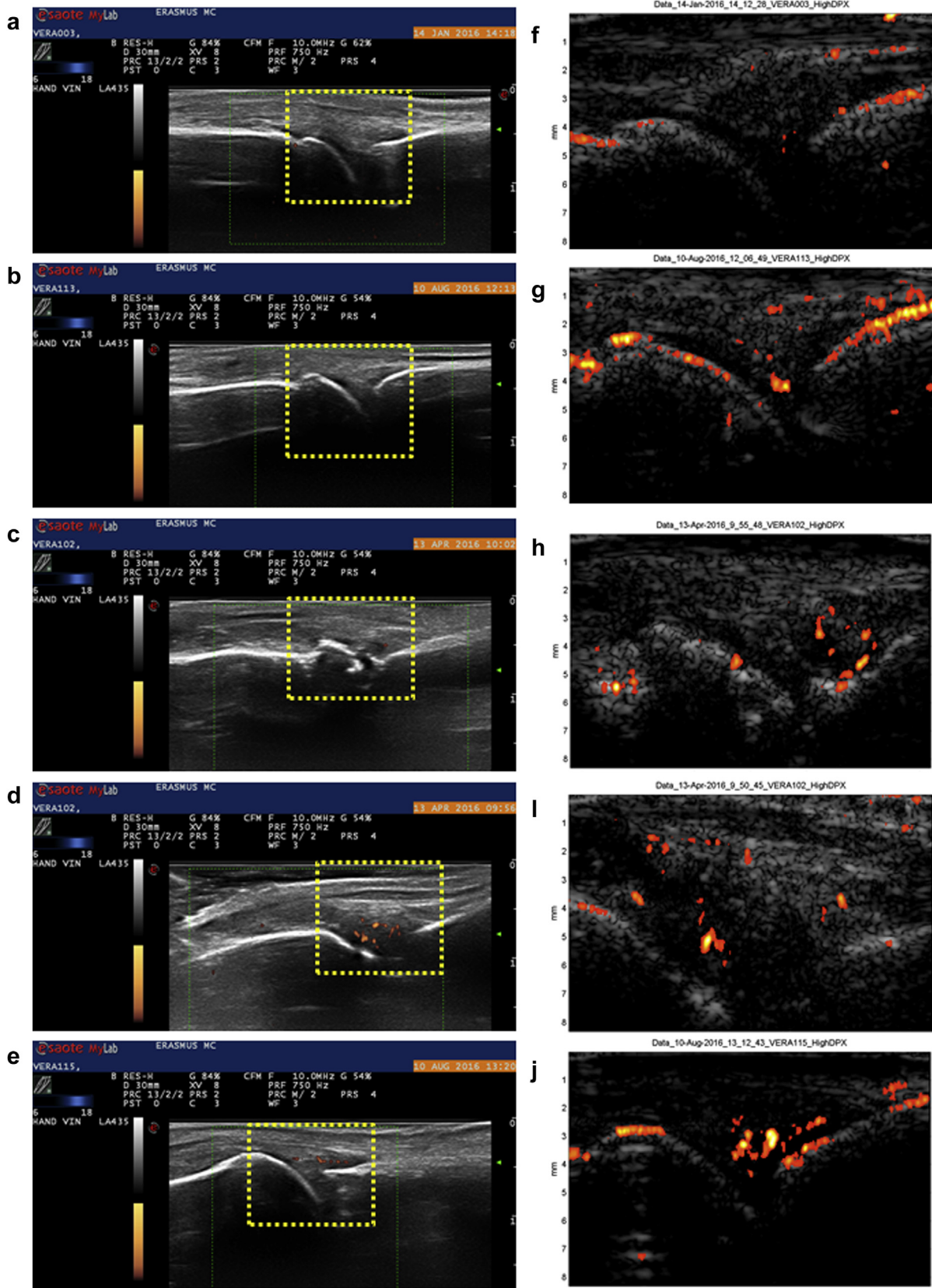
Fig. 4. Metacarpophalangeal joints of healthy controls and RA patients were scanned with conventional PD ultrasound (a–e) and high-frame-rate Doppler imaging (f–j). (a,f) Healthy control. (b,g) RA in remission. (c,h) RA controlled (non-swollen MCP). (d,i) RA controlled (swollen MCP). (e,j) RA flare. The *dashed yellow box* in (a–e) depicts the region of interest in (f–j) with the metacarpal bone (left hand side) and the proximal phalanx. MCP = metacarpophalangeal; RA = rheumatoid arthritis.

(Table 2). PD scores with high-frame-rate ultrasound were significantly different ($p < 0.001$) from PD scores with conventional ultrasound.

Any PD signal detected with conventional ultrasound was also detected with high-frame-rate ultrasound and scored the same PD grade or higher. If no PD signal was detected with conventional ultrasound, high-frame-rate ultrasound detected either no or mild PD signal. Moreover, the largest difference between conventional and high-frame-rate ultrasound is observed in the controls and in the non-swollen joints in the patients with controlled RA. Apparently, the high-frame-rate ultrasound detects increased microvasculature in the joint, compared with the control group. This increased microvasculature is detected neither by the physical examination nor by the conventional power Doppler technique.

Power Doppler images acquired with high-frame-rate ultrasound were scored by four observers independently. The κ statistic for inter-rater reliability was 0.55, which means the agreement between the four observers was moderate (Viera and Garrett 2005).

To investigate the potential grading power of high-frame-rate Doppler, we plotted the distribution of PD scores (range: 0–3) in all patients for each different disease state in Figure 5. Note that for each subject, all three measurements per examined joint were scored, and the median value was taken for the data in Figure 5. In all

cases, at least one of the three recordings had a PD score of 1. In correspondence with the median values listed in Table 2, this plot illustrates a gradual shift in PD score from healthy controls to flaring joints, implying that high-frame-rate Doppler can indeed stage the vascularisation. On the other hand, we observed no difference in vascularisation between the swollen and non-swollen joints with controlled disease.

DISCUSSION

Summary

This study investigated the sensitivity of high-frame-rate PD ultrasound for use in rheumatology practice. In a flow phantom, we could detect lower velocities with the high-frame-rate ultrasound machine (0.26 mm/s) than with the conventional ultrasound machine (0.8 mm/s) in a 0.7-mm vessel with the clinically unrealistic but optimal settings to detect low flow velocities with the clinical scanner. In the proof-of-principle study we detected a positive PD signal in all volunteers, diseased or healthy, with high-frame-rate PD ultrasound. This was opposite to the measurements with conventional PD ultrasound, where no PD signal was observed in the healthy volunteers and in RA patients in clinical remission. In patients with controlled RA, we obtained higher PD scores in both clinically swollen and non-swollen MCP joints
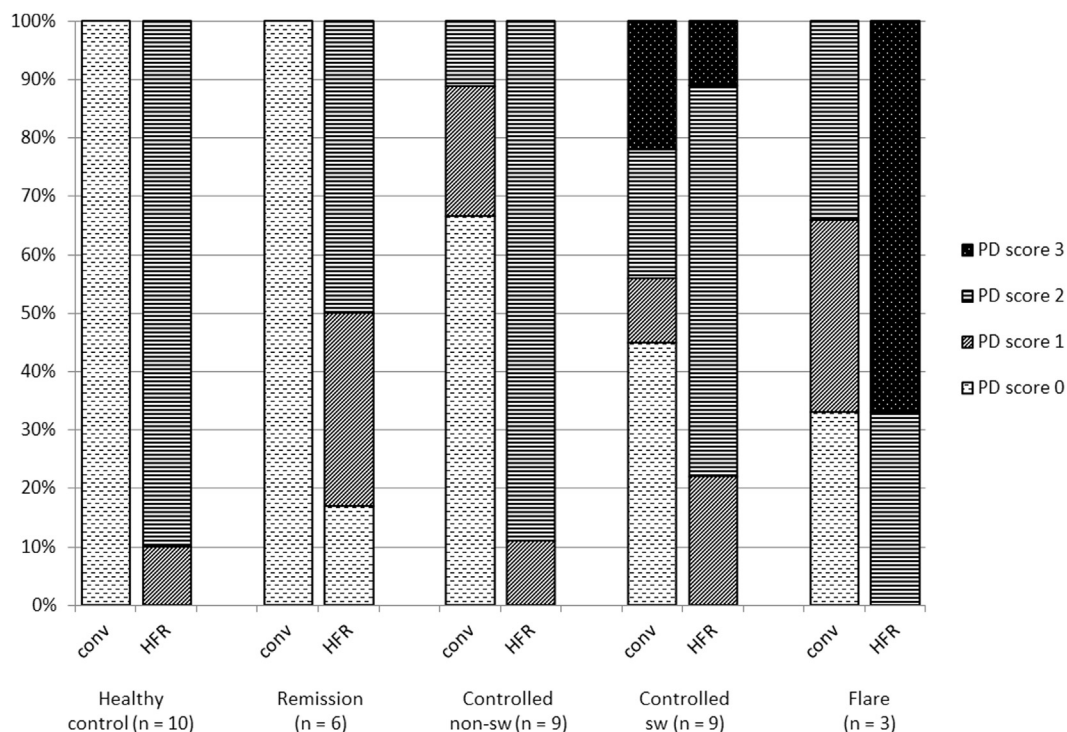

Fig. 5. Distribution of PD scores (range: 0–3) for healthy controls and the RA patient groups for both conventional PD and high-frame rate PD. More active RA coincides with increasing PD score. conv = conventional; HFR = high frame rate; PD = power Doppler; sw = swollen.

with high-frame-rate PD. In RA patients with a clinical flare, PD scores were higher as well with high-frame-rate Doppler than with conventional PD ultrasound. For all groups, PD scores were significantly higher for high-frame-rate ultrasound than for conventional ultrasound. Therefore, high-frame-rate PD ultrasound is a more sensitive tool to detect vascularisation than conventional PD ultrasound.

Clinical implications

These findings have several clinical implications. Firstly, in healthy controls, conventional ultrasound could not detect any PD signal, but with high-frame-rate imaging we found at least median grade 1 PD signal in all controls. These PD signals might refer to normal vascularisation of the synovium, which consists of low velocities not detectable by conventional imaging methods. This finding is consistent with previous research with high-frame-rate Doppler imaging in healthy volunteers by Maresca et al. (2014), although in that study the perfusion was increased by use of a warm water bath in which the hand was held. PD signals in healthy patients in normal clinical circumstances were not included in the conventional grading system (Szkudlarek et al. 2003). Hence, a new grading system which includes PD signals in healthy controls is needed. Such a grading system could be based on estimation of the vessel density (Maresca et al. 2014), although such a method requires careful consideration of the used thresholds. A new grading system could also improve inter-observer agreement, which is important when a new method is introduced into clinical practice. In our study, the agreement was moderate, which could be explained by the semi-quantitative scoring scale, which could introduce subjectivity regarding interpretation especially between grade 1 and grade 2 power Doppler. Anyhow, a study with a larger population is needed to fine-tune the grading of signals on a scale ranging from healthy, through (early) inflammation, to full flare.

Overall, high-frame-rate PD ultrasound was more sensitive in detecting vascularisation, but with some loss of discrimination between healthy controls and RA patients. Further research with high-frame-rate PD ultrasound to improve discrimination might increase our knowledge of the physiology of inflammation, especially the relation between symptoms, clinical swelling, vascularisation and inflammation (Andersen et al. 2014; Kitchen and Kane 2015).

Secondly, in the clinical experiment, we clamped the transducers and mildly fixated the hand to reduce motion from both the ultrasound examiner and the participant. The mechanical arm in which the probe is held may complicate the dissemination. To assess its need, we performed an additional test in which we compared the high-frame-rate PD images recorded with the mechanical arm with those of manual scanning by an expert (M.v.d.V.). Figure 6a,b are two recordings made with the mechanical arm, and Figure 6c,d illustrate manual scanning. There, the bone reflections lead to residual Doppler signals, because of a much higher relative motion of bone and no vasculature detection in the synovium. We quantified peak-to-peak axial motion of 6 μm per recording when scanning with the mechanical arm and 20 μm with manual scanning (mean of 10 recordings each). The different appearances in Figure 6 indicate the need for mechanical stabilization. In the future, the rather large mechanical arm may be replaced by, for example, a dedicated wearable rheumatology probe, which is very gently clipped onto the finger of interest.

We also used the mechanical arm for our *in vivo* measurements with conventional ultrasound to obtain comparable results. In the reported results, we used the same settings (PFR: 750 Hz, wall filter: 3) as in daily clinical practice, leading to presumed equal sensitivity to flow as in daily routine. Yet, with this clamping and hand fixation, we also tested more optimal settings to detect low-flow PD signal (PRF 370 Hz, wall filter 2) without the risk of flash artifacts. Scoring of those images did not lead to results other than those obtained in the main study. Therefore, we have provided the results with the regular clinical settings.

Furthermore, the fact that any examination should give a minor PD signal is highly beneficial for the confidence of the sonographer in the measurement. If no signal is detected, then this is a sign of failure of the measurement, such as malfunctioning (caused by, *e.g.,* broken crystals in the probe), wrong settings or poor acoustic contact between the probe and skin. This is unlike the conventional method, in which "no PD signal" always is interpreted as "no or very minor vascularisation." The conventional ultrasound machine (Esaote MyLab60) is used in daily clinical practice. Although the machine can be considered as mid-range equipment, we selected this machine for comparison as it performed best in detecting low flows in an earlier phantom study (Ten Cate et al. 2013b). We realise that the use of a more recent high-end clinical ultrasound machine might have led to a different result in the comparison. Yet, in a preliminary test with the ultrafast Doppler mode on a Supersonic Imagine Aixplorer with SL15-4 probe, no vascularisation was observed in the metacarpophalangeal joints of a healthy volunteer. As both the Aixplorer ultrafast Doppler and proposed high-frame-rate ultrasound techniques presumably have similar data acquisition schemes, the difference in sensitivity may be sought in either the choice of probe (the currently used probe has a more shallow elevation focus than the probe of
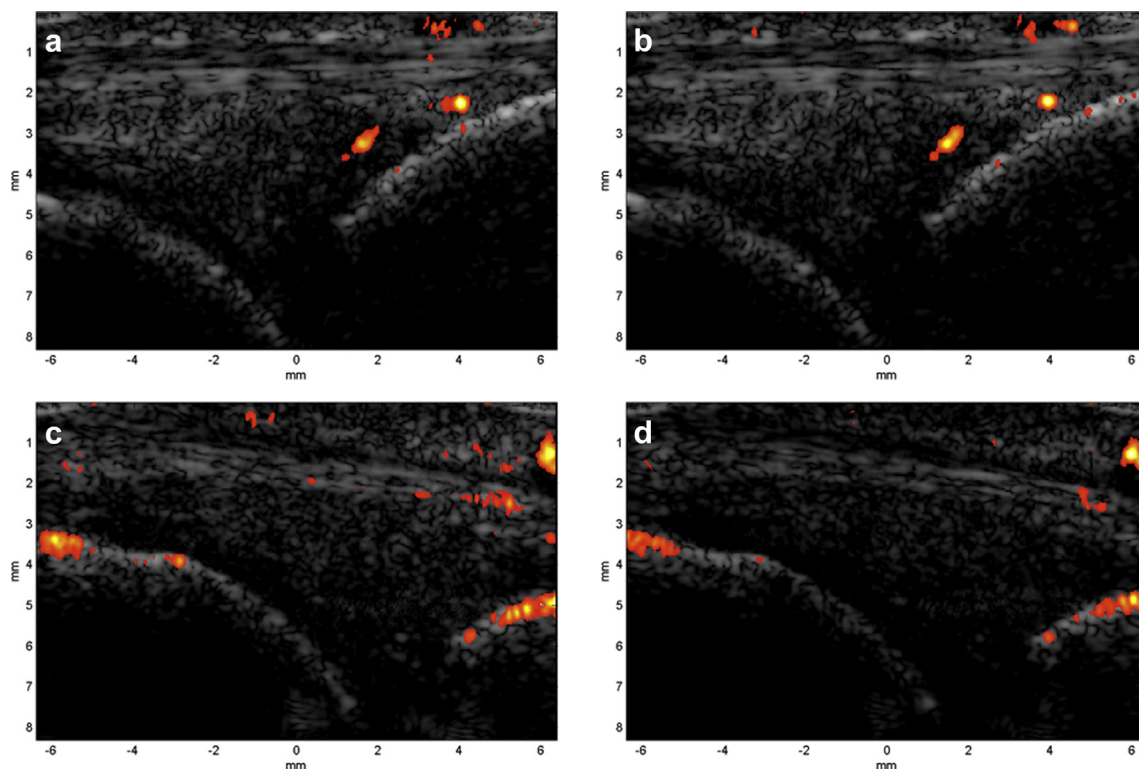
Fig. 6. Variability of power Doppler signals when the probe was held in the hydrostatic arm (a,b) and when manually held (c,d).

the Aixplorer) or the use of the SVD scheme to cancel tissue signals, thus allowing for more sensitive settings.

Methodology

As there is no gold standard for imaging the microvasculature in finger joints in RA patients, we first investigated the technique with the flow phantom, establishing actual detection of very slow flows. Second, to investigate whether the Doppler signal is "real" *in vivo*, we repeated the measurement 10 times at the same location of the MCP joint of one healthy volunteer. It appeared that the same vessels always appeared, and no other appeared, except for isolated pixels at the level of the bone reflection. See Figure 6a,b for two example images. The pixel difference would certainly not change the scoring of such image. SVD has been used to suppress tissue signals before in high-frame-rate Doppler (Demené et al. 2015; Song et al. 2017), and similar to Demené et al., we optimised the choice of the singular values that are supposed to contain blood flow information. By visual inspection of the resulting PD images, we found that most blood flow information was contained in the SVD singular values 5 to 32 (of 122 maximum). Yet, minimal bone motion also led to a PD signal in the lower values (range: 5–15, roughly). In such a case, minimal motion of a large scattering object such as the

hard boundary of bone produces a PD signal similar to that of blood flow, which is characterised by a large motion of a low scattering object. Therefore, we analysed the PD frames obtained with singular values 18 to 32. Different sets of SVD components, in which the pixel colouring threshold and colour priority were also manually varied, exhibited minor differences in appearance in terms of noise and bone signal. Yet, this did not lead to a different staging, because the observer in this series (M.v.d.V.) was used to interpreting bone signal and noise as artefacts. Any automated analysis algorithms that may be used to stage the vascularisation should be devised to perform this discrimination based on the anatomic landmarks present in the grey-scale images and PD data.

Retrospectively, we also processed the high-frame-rate raw data with a conventional wall filter with relatively low cutoff frequency (37.5 Hz, corresponding to 2.4 mm/s flow velocity). This resulted in very large signal from bone and no detection of blood flow in cases where filtering with SVD resulted in minor but persistent detection. Lower cutoff values resulted in large flash artefacts and bone signals. This result is consistent with that provided by Demené et al. (2015) on the comparison between SVD and conventional wall filtering. The SVD filtering technique removes the tissue motion that is

spatially coherent in the images, independent of the typical Doppler frequency of that motion. Because spatial coherency has no influence on conventional wall filtering, the bone signal is not sufficiently suppressed by that wall filter.

In conventional applications, the Doppler power is scaled by the local B-mode intensity (so-called colour priority). Although this suppresses the spurious Doppler signal from bone, it may also enhance Doppler signal from hypo-echoic regions in the joint such as those illustrated in Figure 4e, thus resulting in a blooming effect and perhaps overestimating tissue motion. We therefore did not apply the scaling of the Doppler power by the B-mode intensity in the final data analysis.

Because we are processing the data in "power Doppler" mode in which, basically, any signal variation (after tissue removal) is integrated and imaged, there is no intrinsic limitation of maximum detectable blood flow. Therefore, 125 Hz will not limit the maximum detectable flow velocities. Note that this is opposite the situation with colour Doppler or pulsed wave Doppler, in which aliasing (caused by too low a PRF) affects the sign and magnitude of flow velocity estimation dramatically.

Our relatively quick implementation of the complementary grey-scale images led to a poor grey-scale resolution compared with that of conventional ultrasound imaging. This shortcoming can be solved in the future by increasing the number of angles of plane waves for reconstructing the grey-scale image, or even by using conventional line scanning, without dramatic increase in the overall recording time.

REFERENCES

Aletaha D, Neogi T, Silman AJ, Funovits J, Felson DT, Bingham CO III, Birnbaum NS, Burmester GR, Bykerk VP, Cohen MD, Combe B, Costenbader KH, Dougados M, Emery P, Ferraccioli G, Hazes JM, Hobbs K, Huizinga TW, Kavanaugh A, Kay J, Kvien TK, Laing T, Mease P, Menard HA, Moreland LW, Naden RL, Pincus T, Smolen JS, Stanislawska-Biernat E, Symmons D, Tak PP, Upchurch KS, Vencovsky J, Wolfe F, Hawker G. Rheumatoid arthritis classification criteria: An American College of Rheumatology/European League Against Rheumatism collaborative initiative. Arthritis Rheum 2010;62:2569–2581.

Andersen M, Ellegaard K, Hebsgaard JB, Christensen R, Torp-Pedersen S, Kvist PH, Soe N, Romer J, Vendel N, Bartels EM, Danneskiold-Samsoe B, Bliddal H. Ultrasound colour Doppler is associated with synovial pathology in biopsies from hand joints in rheumatoid arthritis patients: A cross-sectional study. Ann Rheum Dis 2014;73:678–683.

Backhaus M, Burmester GR, Gerber T, Grassi W, Machold KP, Swen WA, Wakefield RJ, Manger B. Guidelines for musculoskeletal ultrasound in rheumatology. Ann Rheum Dis 2001;60:641–649.

Bercoff J, Montaldo G, Loupas T, Savery D, Mézière F, Fink M, Tanter M. Ultrafast compound Doppler imaging: Providing full blood flow characterization. IEEE Trans Ultrason Ferroelectr Freq Control 2011;58:134–147.

Brown AK, Quinn MA, Karim Z, Conaghan PG, Peterfy CG, Hensor E, Wakefield RJ, O'Connor PJ, Emery P. Presence of significant synovitis in rheumatoid arthritis patients with disease-modifying antirheumatic drug-induced clinical remission: Evidence from an imaging study may explain structural progression. Arthritis Rheum 2006;54:3761–3773.

Brown AK, Conaghan PG, Karim Z, Quinn MA, Ikeda K, Peterfy CG, Hensor E, Wakefield RJ, O'Connor PJ, Emery P. An explanation for the apparent dissociation between clinical remission and continued structural deterioration in rheumatoid arthritis. Arthritis Rheum 2008;58:2958–2967.

Demené C, Pernot M, Biran V, Alison M, Fink M, Baud O, Tanter M. Ultrafast Doppler reveals the mapping of cerebral vascular resistivity in neonates. J Cerebral Blood Flow Metab 2014;34:1009–1017.

Demené C, Deffieux T, Pernot M, Osmanski BF, Biran V, Gennisson JL, Sieu LA, Bergel A, Franqui S, Correas JM, Cohen I, Baud O, Tanter M. Spatiotemporal clutter filtering of ultrafast ultrasound data highly increases Doppler and fultrasound sensitivity. IEEE Trans Med Imaging 2015;34:2271–2285.

Demené C, Tiran E, Sieu LA, Bergel A, Gennisson JL, Pernot M, Deffieux T, Cohen I, Tanter M. 4D microvascular imaging based on ultrafast Doppler tomography. NeuroImage 2016;127:472–483.

Ekroll IK, Voormolen MM, Standal OKV, Rau JM, Lovstakken L. Coherent compounding in Doppler imaging. IEEE Trans Ultras Ferroelectr Freq Control 2015;62:1634–1643.

Evans DH, McDicken WN. Doppler ultrasound: Physics, instrumentation and signal processing. New York: Wiley; 1999.

Filer A, de Pablo P, Allen G, Nightingale P, Jordan A, Jobanputra P, Bowman S, Buckley CD, Raza K. Utility of ultrasound joint counts in the prediction of rheumatoid arthritis in patients with very early synovitis. Ann Rheum Dis 2011;70:500–507.

Hasegawa H, Kanai H. Simultaneous imaging of artery-wall strain and blood flow by high frame rate acquisition of RF signals. IEEE Trans Ultrason Ferroelectr Freq Control 2008;55:2626–2639.

Kitchen J, Kane D. Greyscale and power Doppler ultrasonographic evaluation of normal synovial joints: Correlation with pro- and antiinflammatory cytokines and angiogenic factors. Rheumatology (Oxford) 2015;54:458–462.

Lenge M, Ramalli A, Boni E, Liebgott H, Cachard C, Tortoli P. Highframe-rate 2-D vector blood flow imaging in the frequency domain. IEEE Trans Ultras Ferroelectr Freq Control 2014;61:1504–1514.

Maresca D, Tanter M, Pernot M. Ultrasound microangiography of the metacarophalangeal joint using ultrafast Doppler. Proc IEEE Int Ultrason Symp 2014;425–427.

McInnes IB, Schett G. The pathogenesis of rheumatoid arthritis. N Engl J Med 2011;365:2205–2219.

Peluso G, Michelutti A, Bosello S, Gremese E, Tolusso B, Ferraccioli G. Clinical and ultrasonographic remission determines different chances of relapse in early and long standing rheumatoid arthritis. Ann Rheum Dis 2011;70:172–175.

Prevoo ML, van 't Hof MA, Kuper HH, van Leeuwen MA, van de Putte LB, van Riel PL. Modified disease activity scores that include twenty-eight-joint counts. Development and validation in a prospective longitudinal study of patients with rheumatoid arthritis. Arthritis Rheum 1995;38:44–48.

Ramnarine KV, Nassiri DK, Hoskins PR, Lubbers J. Validation of a new blood-mimicking fluid for use in Doppler flow test objects. Ultrasound Med Biol 1998;24:451–459.

Saleem B, Brown AK, Quinn M, Karim Z, Hensor EM, Conaghan P, Peterfy C, Wakefield RJ, Emery P. Can flare be predicted in DMARD treated RA patients in remission, and is it important? A cohort study. Ann Rheum Dis 2012;71:1316–1321.

Scire CA, Montecucco C, Codullo V, Epis O, Todoerti M, Caporali R. Ultrasonographic evaluation of joint involvement in early rheumatoid arthritis in clinical remission: Power Doppler signal predicts short-term relapse. Rheumatology (Oxford) 2009;48:1092–1097.

Silman AJ, Pearson JE. Epidemiology and genetics of rheumatoid arthritis. Arthritis Res 2002;4(Suppl 3):S265–S272.

Smolen JS, Breedveld FC, Eberl G, Jones I, Leeming M, Wylie GL, Kirkpatrick J. Validity and reliability of the twenty-eight-joint count for the assessment of rheumatoid arthritis activity. Arthritis Rheum 1995;38:38–43.

Song P, Manduca A, Trzasko J, Chen S. Ultrasound small vessel imaging with block-wise adaptive local clutter filtering. IEEE Trans Med Imaging 2017;36:251–262.

Stoffer MA, Schoels MM, Smolen JS, Aletaha D, Breedveld FC, Burmester G, Bykerk V, Dougados M, Emery P, Haraoui B, Gomez-Reino J, Kvien TK, Nash P, Navarro-Compan V, Scholte-Voshaar M, van Vollenhoven R, van der Heijde D, Stamm TA. Evidence for treating rheumatoid arthritis to target: Results of a systematic literature search update. Ann Rheum Dis 2015; 75:16–22.

Szkudlarek M, Court-Payen M, Jacobsen S, Klarlund M, Thomsen HS, Ostergaard M. Interobserver agreement in ultrasonography of the finger and toe joints in rheumatoid arthritis. Arthritis Rheum 2003; 48:955–962.

Tanter M, Fink M. Ultrafast imaging in biomedical ultrasound. IEEE Trans Ultrason Ferroelectr Freq Control 2014;61:102–119.

Teirlinck CJ, Bezemer RA, Kollmann C, Lubbers J, Hoskins PR, Ramnarine KV, Fish P, Fredeldt KE, Schaarschmidt UG. Development of an example flow test object and comparison of five of these test objects, constructed in various laboratories. Ultrasonics 1998; 36:653–660.

Ten Cate DF, Luime JJ, Swen N, Gerards AH, De Jager MH, Basoski NM, Hazes JM, Haagsma CJ, Jacobs JW. Role of ultrasonography in diagnosing early rheumatoid arthritis and remission of rheumatoid arthritis: A systematic review of the literature. Arthritis Res Ther 2013a;15:R4.

Ten Cate DF, Luime JJ, van der Ven M, Hazes JM, Kooiman K, de Jong N, Bosch JG. Very different performance of the power Doppler modalities of several ultrasound machines ascertained by a microvessel flow phantom. Arthritis Res Ther 2013b;15: R162.

Torp-Pedersen ST, Terslev L. Settings and artefacts relevant in colour/ power Doppler ultrasound in rheumatology. Ann Rheum Dis 2008; 67:143–149.

van Nies JA, Krabben A, Schoones JW, Huizinga TW, Kloppenburg M, van der Helm-van Mil AH. What is the evidence for the presence of a therapeutic window of opportunity in rheumatoid arthritis? A systematic literature review. Ann Rheum Dis 2014;73:861–870.

Viera AJ, Garrett JM. Understanding interobserver agreement: The kappa statistic. Fam Med 2005;37:360–363.

Yoshimi R, Hama M, Takase K, Ihata A, Kishimoto D, Terauchi K, Watanabe R, Uehara T, Samukawa S, Ueda A, Takeno M, Ishigatsubo Y. Ultrasonography is a potent tool for the prediction of progressive joint destruction during clinical remission of rheumatoid arthritis. Mod Rheumatol 2013;23:456–465.